Boundary Integral Equations for Recovery of Design Sensitivities in Shape Optimization

M. R. Barone* and R. J. Yang†
General Motors Research Laboratories, Warren, Michigan

A new formulation for obtaining design sensitivities in shape optimization has been developed. The formulation is based on a direct application of the material derivative concept to the appropriate boundary integral equations for displacements and stresses in an elastic solid. As a check on accuracy, the approach was applied to a uniformly loaded infinite plate containing an elliptical hole. In this case, the availability of an analytical solution made it possible to calculate errors exactly. Furthermore, a wide range of stress states could be considered simply by varying the aspect ratio of the elliptical hole. For convenience, the design sensitivities were calculated with respect to changes in the major axis. Numerical convergence was established by comparing results based on four successive boundary meshes. In general, the predictions for both displacement and stress sensitivities were remarkably accurate.

Introduction

CURRENT interest in structural shape optimization is motivated largely by increased demands for more cost-competitive designs. Since most optimal design procedures involve repeated finite-element analyses, large-scale implementation can be extremely costly. Computational costs can be particularly prohibitive in shape optimization, where a new mesh is required for each trial design. The need to minimize or control such costs has fostered major advances in the area of automated mesh generation.[1,2] It has also provided the basic incentive for considering the boundary-element method in shape optimization.[3-9] In the latter case, the mesh generation is relatively straightforward and inexpensive because the discretization is confined to the boundary. On the other hand, the system matrices are unsymmetric and fully dense. Therefore, the advantage of less expensive remeshing may be offset by higher solution costs unless proper care is exercised. Obviously, over-refinement should be avoided and substructuring used whenever appropriate. Considerable savings can also be realized by taking advantage of recovery procedures for design sensitivities that eliminate the need for redundant matrix inversions. This paper concerns the development and evaluation of recovery procedures for design sensitivities that follow directly from the primitive integral equations for displacements and stresses on the boundary.

Considerable effort has been devoted to developing efficient techniques for evaluating design sensitivities in the context of the finite-element method.[10-14] Of the existing finite-element-based techniques, the adjoint variable approach and the implicit differentiation method appear best suited for implementation in a boundary-element context. The adjoint variable technique has been used by Mota Soares,[5] Choi,[6] and Meric[7] in a variety of boundary-element applications. Although the formal adaptation of this technique is conceptually straightforward, major computational difficulties arise when evaluating displacement and stress sensitivities at discrete points. The problem stems from the fact that the adjoint solutions for these two cases correspond to a concentrated force and moment, respectively. Strictly speaking, these solutions cannot be expressed in terms of the boundary-element formulation because they give rise to unbounded integrals. One remedy[5] is to represent the concentrated force or moment by a statically equivalent bounded load distribution. Although some empirical guidelines for selecting load distributions have been suggested in Ref. 5, the success of such schemes has been marginal, especially in evaluating stress sensitivities.

In contrast to the adjoint variable method, the determination of design sensitivities by implicit differentiation of system matrices is a relatively straightforward process. Recently, Wu[8] employed a boundary-element version of the implicit method to solve several interesting two- and three-dimensional design problems. In this case, the derivative of the system matrix was approximated by a finite difference. Although he was able to show convergence of the solutions in the examples considered, the effect of the finite-difference interval on convergence in more general applications is still in question. An effective alternative to the finite-difference algorithm in Ref. 8 was developed concurrently by Kane,[9] who generated the desired sensitivities by differentiating the system matrix analytically. Ultimately, however, this technique requires a direct differentiation of the approximate shape functions used to represent both the field variables and coordinate geometry on the boundary. Despite the basic appeal of Kane's approach, the "load" point must be placed outside the region to avoid singular integrations. Besides being somewhat arbitrary, this strategic adjustment appears to introduce unwarranted complications. First, the element closest to the singular (load) point is divided into eight subregions of varying length to accommodate the sharply varying, albeit regular, kernels. Although a total of 33 nonuniformly space sampling points proved adequate in the examples considered, it was necessary to modify the distribution to accommodate changes in the position of the singularity. Furthermore, hundreds of sampling points were required when attempts were made to distribute them uniformly. Although a load point offset of about 1% was reported to work best in the applications considered in Ref. 9, the prospects for success in problems characterized by more severe stress raisers are uncertain.

In this paper, we develop analytical expressions for design sensitivities by differentiating the basic integral equation for displacements on the boundary directly as well as the corresponding stress recovery equation developed by Cruse.[15] One of the advantages of this approach is it avoids the sensitive process of determining singular adjoint solutions numerically.[5-7] Unlike the technique proposed in Ref. 9, there is no need to differentiate field variable shape functions in deter-

Received May 1, 1987; revision received Nov. 16, 1987. Copyright © American Institute of Aeronautics and Astronautics, Inc., 1988. All rights reserved.

*Senior Staff Research Engineer, Engineering Mechanics Department.

†Senior Research Engineer, Engineering Mechanics Department. Senior Research Scientist, Aero-Astronautics Group.

mining stress sensitivities. Instead, the differentiation is done analytically before performing the final quadrature, thereby avoiding unnecessary numerical errors. An additional improvement in numerical implementation is accomplished by using a special identity to remove all singular integrals from the equations for displacement sensitivities, save those that normally appear in the conventional boundary integral equations. In an effort to entirely avoid singular integrals in the equation for stress sensitivities, we consider a second formulation based on an eigenfunction extraction technique. This technique was first developed by Barone and Robinson[16] for determining stress fields near corners and cracks. Later Vasilopoulos[17] used a finite-element adaptation of this approach to recover stresses at regular boundary points.

In contrast to the approach taken in Ref. 9, the proposed recovery integrals were evaluated with the singular (load) point on the boundary. This not only eliminates the arbitrariness in locating the singularity but does so without adding to the computational burden. In fact, the numerical implementation of the resulting expressions involves little more than the standard discretization used in conventional boundary integral applications. Although the basic equations are developed in the context of two-dimensional elasticity problems, it is possible to derive the corresponding three-dimensional expressions without introducing new concepts. Since the integration procedures required for effective implementation differ significantly from the two-dimensional counterpart, computational details pertaining to three-dimensional applications will be considered in a future paper.

A review of the basic boundary integral equations for two-dimensional plane-strain problems is provided in the next section. This is followed by a derivation of the corresponding recovery integrals for displacement sensitivities. We then show how the numerical treatment of these expressions can be simplified by applying a special identity to eliminate unnecessary singular integrals. Next, two different recovery equations are developed for stress sensitivities. One follows directly from Somigliana's identity, and the other is based on the eigenvalue extraction technique for boundary stresses mentioned earlier. Finally, the recovery process is applied to an example problem of an infinite two-dimensional plate with an elliptical hole. Numerical predictions generated for different mesh spacings are compared to analytical results based on the exact plane-strain solution. The effect of geometry is determined by repeating the analysis with aspect ratios for the hole boundaries of 1, 4, and 8, which correspond to stress concentrations of 3, 9, and 17, respectively. Computing design sensitivities for this extreme range in stress concentration serves as a rigorous test for the method.

Design Sensitivity Analysis

Consider a two-dimensional elastic solid R subject to prescribed displacements u_α and/or tractions t_α on the boundary ∂R. (Greek subscripts or superscripts take the values 1, 2, and summation is implied over repeated indices in the usual manner.) In this case, Somigliana's integral identity[18,19] for the displacement u_κ at point y can be expressed as

$$\Lambda u_\kappa(y) = \int_{\partial R} [t_\alpha(x) u_\alpha^\kappa(x,y) - u_\alpha(x) t_\alpha^\kappa(x,y)]\, ds(x)$$

$$\Lambda = \begin{cases} 1: & y \in R \\ \frac{1}{2}: & y \in \partial R \end{cases} \tag{1}$$

where $x \in \partial R$ is the field point and $ds(x)$ the associated element of arc length. If we consider the plane-strain case and let μ and ν denote the shear modulus and Poisson's ratio, respectively, then

$$u_\alpha^\kappa = -\frac{1}{8\pi\mu(1-\nu)} [(3-4\nu)\delta_{\kappa\alpha} \log(r) - r_{,\alpha} r_{,\kappa}]$$

$$t_\alpha^\kappa = -\frac{1}{4\pi\mu(1-\nu)r} \{(1-2\nu)(n_{,\kappa} r_{,\alpha} - n_{,\alpha} r_{,\kappa}) + [(1-2\nu)\delta_{\kappa\alpha} + 2r_{,\alpha} r_{,\kappa}] r_{,n}\} \tag{2}$$

where $r = |x - y|$, $(\,)_{,\alpha} = \partial(\,)/\partial x_\alpha$, and n is the outward unit normal. These kernels are the well-known fundamental (Kelvin) solutions associated with two concentrated loads acting in mutually perpendicular directions ($\kappa = 1, 2$) at the point y.

Equation (1) forms the basis for the ensuing design sensitivity analysis. Although this analysis focuses on the determination of sensitivities at boundary points, the basic equations are also valid when $y \in R$. Clearly there is no need to dwell on the latter case, since all related integrations are regular and can be carried out routinely. Moreover, the critical displacements and stresses usually occur on the boundary.

It is assumed in developing the recovery integrals for design sensitivities that shape changes occur continously. To simplify the development, let the finite-dimensional vector b represent the shape of the region R. Then Eq. (1) can be rewritten as

$$\Lambda u_\kappa(b,y) = \int_{\partial R} [t_\alpha(b,x) u_\alpha^\kappa(x,y) - u_\alpha(b,x) t_\alpha^\kappa(b,x,y)]\, ds(b,x) \tag{3}$$

where t_α^κ, unlike u_α^κ, is a function of b because it depends explicitly on the unit normal n. After taking the total derivative of Eq. (3) with respect to the design variable b_i, we obtain

$$\Lambda \dot{u}_\kappa(b,y) = \int_{\partial R} [\dot{t}_\alpha(b,x) u_\alpha^\kappa(x,y) - \dot{u}_\alpha(b,x) t_\alpha^\kappa(b,x,y)]\, ds(b,x) + \int_{\partial R} [t_\alpha(b,x) \dot{u}_\alpha^\kappa(x,y) - u_\alpha(b,x) \dot{t}_\alpha^\kappa(b,x,y)]\, ds(b,x) + \int_{\partial R} [t_\alpha(b,x) u_\alpha^\kappa(x,y) - u_\alpha(b,x) t_\alpha^\kappa(b,x,y)]\, \dot{ds}(b,x) \tag{4}$$

where $(\dot{\cdot})$ denotes $\mathrm{d}(\,)/\mathrm{d}b_i$, $\dot{ds} = (\dot{x}_{\beta,\beta} - n_\alpha n_\beta \dot{x}_{\alpha,\beta}) ds$[10,11] and

$$\dot{u}_\alpha^\kappa(x,y) = u_{\alpha,\gamma}^\kappa(x,y) \left(\frac{\partial x_\gamma}{\partial b_i} - \frac{\partial y_\gamma}{\partial b_i}\right)$$

$$\dot{t}_\alpha^\kappa(b,x,y) = \frac{\mathrm{d}}{\mathrm{d}b_i} [\sigma_{\alpha\beta}^\kappa(x,y) n_\beta(b,x)] = \sigma_{\alpha\beta,\gamma}^\kappa(x,y) \left(\frac{\partial x_\gamma}{\partial b_i} - \frac{\partial y_\gamma}{\partial b_i}\right) n_\beta(b,x) + \sigma_{\alpha\beta}^\kappa \dot{n}_\beta(b,x) \tag{5}$$

The minus sign in Eq. (5) occurs because differentiating either kernel with respect to y_α instead of x_α changes the sign of the resulting gradient. If we associate the design change with a physical deformation and equate b_i with time, then $(\dot{\cdot})$ is formally equivalent to a material derivative.

Although the recovery of displacement and traction sensitivities from Eq. (4) is conceptually straightforward, it is helpful in developing an effective computational approach to consider first the asymptotic character of the corresponding integrands as $x \to y$. It follows from the usual small argument

expansions for the kernels in Eq. (2) that

$$u_\alpha^\kappa = O[\log(s)]$$
$$u_{\alpha,\gamma}^\kappa = O(1/s)$$
$$\sigma_{\alpha\beta}^\kappa = O(1/s)$$
$$\sigma_{\alpha\beta,\gamma}^\kappa = O(1/s^2) \tag{6}$$

where s is the arc length coordinate of x measured from y. A similar expansion of the local geometry gives

$$\frac{\partial x_\gamma}{\partial b_i} - \frac{\partial y_\gamma}{\partial b_i} = O(s) \tag{7}$$

As indicated previously, Eq. (7) is based on the assumption of continuous design or geometric perturbations. If we regard such perturbations as physical deformations, then all motions are admissible, except those that induce rupture. Clearly this level of generality is consistent with the concept of *continuum* shape optimization.[10]

After substituting Eqs. (5-7) in Eq. (4), we observe that the resulting integrands are $O(1/s)$. Although special techniques[19,20] can be used to determine the corresponding Cauchy principal values, they are usually considerably less convenient to implement than routine Gauss quadrature. In this case, however, it is possible to simplify the computations by recasting Eq. (4) in a more appropriate form. First consider an arbitrary rigid body translation where u_α^R = constant in R and all admissible design perturbations $R + \delta R$. Replacing $\dot{u}_\kappa$ in Eq. (4) by this special solution yields the identity

$$\int_{\partial R} [u_\alpha^R \, \dot{t}_\alpha^\kappa(x,y)]\mathrm{d}s(x) + \int_{\partial R} [u_\alpha^R \, t_\alpha^\kappa(b,x,y)]\dot{\mathrm{d}}s(b,x) = 0 \tag{8}$$

Subtracting Eq. (8) from Eq. (4) gives

$$\begin{aligned}\Lambda\dot{u}_\kappa(y) = &\int_{\partial R} [\dot{t}_\alpha(b,x)u_\alpha^\kappa(x,y) - \dot{u}_\alpha(b,x)t_\alpha^\kappa(b,x,y)]\,\mathrm{d}s(b,x)\\ &+ \int_{\partial R} [t_\alpha(b,x)\dot{u}_\alpha^\kappa(x,y) - \bar{u}_\alpha(b,x)\dot{t}_\alpha^\kappa(b,x,y)]\,\mathrm{d}s(b,x)\\ &+ \int_{\partial R} [t_\alpha(b,x)u_\alpha^\kappa(x,y) - \bar{u}_\alpha(b,x)t_\alpha^\kappa(b,x,y)]\,\dot{\mathrm{d}}s(b,x)\end{aligned} \tag{9}$$

where $\bar{u}_\alpha(b,x) = u_\alpha(b,x) - u_\alpha^R$. Next we let $u_\alpha^R = u_\alpha(b,y)$ so that $\bar{u}_\alpha = O(s)$ when $x \to y$. Now it follows from Eqs. (5-8) that the last two integrals in Eq. (9) are regular and can be evaluted using standard Gauss quadrature. Except for a difference in field variables, the first line in Eq. (9) is identical to the basic boundary integral equation, Eq. (3). Hence, the same standard numerical procedures employed in the solution of Eq. (3) can be used to solve Eq. (9) for $\dot{u}_\kappa$ and/or $\dot{t}_\kappa$. Furthermore, there is no need for additional matrix inversions once Eq. (3) is solved, because the coefficient matrices associated with u_κ, t_κ and $\dot{u}_\kappa$, $\dot{t}_\kappa$ are identical.

An appealing feature of the recovery process embodied in Eq. (9) is that all derivatives are evaluated analytically prior to discretization. Although it is possible to retain this advantage in stress sensitivity analyses, the choice of a suitable primitive recovery equation for the boundary stress $\sigma_{\alpha\beta}$ is less obvious. Two equally admissible but very different representations for stress are considered in this paper. The first was introduced by Cruse[15] in the context of fracture mechanics and can be derived by substituting Eq. (3) into the constitutive equations for plane strain and removing a rigid body motion. After rewriting the expression in Ref. 15 to reflect the proper dependence on the design vector b we obtain

$$\begin{aligned}\Lambda\sigma_{\alpha\beta}(b,y) = \int_{\partial R} &[t_\gamma(b,x)D_{\gamma\alpha\beta}(x,y)\\ &- \bar{u}_\gamma(b,x)S_{\gamma\alpha\beta}(b,x,y)]\,\mathrm{d}s(b,x)\end{aligned} \tag{10}$$

where

$$D_{\gamma\alpha\beta} = \frac{1}{4\pi(1-\nu)r}\,[(1-2\nu)(r_{,\alpha}\delta_{\beta\gamma} + r_{,\beta}\delta_{\alpha\gamma} - r_{,\gamma}\delta_{\alpha\beta}) + 2r_{,\alpha}r_{,\beta}r_{,\gamma}]$$

$$\begin{aligned}S_{\gamma\alpha\beta} = \frac{\mu}{2\pi(1-\nu)r^2}\Big\{&2r_{,n}[(1-2\nu)\delta_{\alpha\beta}r_{,\gamma}\\ &+ \nu(\delta_{\beta\gamma}r_{,\alpha} + \delta_{\alpha\gamma}r_{,\beta}) - 4r_{,\alpha}r_{,\beta}r_{,\gamma}]\\ &+ 2\nu(n_\alpha r_{,\beta}r_{,\gamma} + n_\beta r_{,\alpha}r_{,\gamma}) - (1-4\nu)n_\gamma\delta_{\alpha\beta}\\ &+ (1-2\nu)(2n_\gamma r_{,\alpha}r_{,\beta} + n_\beta\delta_{\alpha\gamma} + n_\alpha\delta_{\beta\gamma})\Big\}\end{aligned} \tag{11}$$

Differentiation of Eq. (10) with respect to b_i yields the corresponding expression for stress sensitivity

$$\begin{aligned}&\Lambda\dot{\sigma}_{\alpha\beta}(b,y)\\ &= \int_{\partial R} [\dot{t}_\gamma(b,x)D_{\gamma\alpha\beta}(x,y) - \dot{\bar{u}}_\gamma(b,x)S_{\gamma\alpha\beta}(b,x,y)]\mathrm{d}s(b,x)\\ &+ \int_{\partial R} [t_\gamma(b,x)\dot{D}_{\gamma\alpha\beta}(x,y) - \bar{u}_\gamma(b,x)\dot{S}_{\gamma\alpha\beta}(b,x,y)]\mathrm{d}s(b,x)\\ &+ \int_{\partial R} [t_\gamma(b,x)D_{\gamma\alpha\beta}(x,y) - \bar{u}_\gamma(b,x)S_{\gamma\alpha\beta}(b,x,y)]\dot{\mathrm{d}}s(b,x)\end{aligned} \tag{12}$$

It follows from Eqs. (7) and (11) that the integrals in Eqs. (10) and (12) contain terms of $O(1/s)$ like those that appear in the basic integral equation, Eq. (3), for displacements and tractions on the boundary. In the former case, however, the simple rigid body displacement technique[18,19] for evaluating Cauchy principal values indirectly does not apply. Therefore, a method developed by Kutt[19,20] for finite-part integration was employed in the example problem considered in the next section.

Recently, Vasilopoulos[17] proposed an eigenfunction extraction procedure for stress recovery that eliminates the need for singular integrations when the boundary conditions are homogeneous. This approach is based on integral equations first developed by Barone and Robinson[16] for determining stresses at corners of arbitrary angle α. Letting $\alpha = \pi$ in the general formulation produces the desired stress recovery equation. In this case, the local stress field at y is determined by the leading term of an eigenfunction expansion, which is known a priori except for a multiplicative stress parameter K. After removing the rigid body motion $u_\alpha^R = u_\alpha(b,y)$ in the usual way, the integral equations for K[16,17] can be expressed as

$$K(y,b) = \int_{\partial R} [t_\alpha(b,x)u_\alpha^*(x,y) - \bar{u}_\alpha(b,x)t_\alpha^*(b,x,y)]\mathrm{d}s(b,x) \tag{13}$$

where u_α^* and t_α^* are special kernels derived from eigensolutions to the infinite elastic wedge problem that satisfy the appropriate homogeneous boundary conditions. As long as the actual boundary conditions at y are the same, the integrands in Eq. (13) remain bounded. Usually, the solutions for u_α^* and t_α^* are expressed in polar form.[21] For the traction-

free case considered in this paper,

$$u_\rho^* = 4\rho^{-1}(1-4/\nu)\cos\varphi$$

$$u_\varphi^* = -2\rho^{-1}(2-1/\nu)\sin\varphi$$

$$\sigma_\rho^* = \frac{8\mu}{\nu}\rho^{-2}\cos\varphi$$

$$\sigma_\varphi^* = 0$$

$$\sigma_{\rho\varphi}^* = \frac{8\mu}{\nu}\rho^{-2}\sin\varphi\cos\varphi \tag{14}$$

where ρ and φ are polar coordinates. The corresponding stresses at y with $\varphi = 0$ are

$$\sigma_\rho = -(8\mu/\nu)K$$

$$\sigma_\varphi = \sigma_{\rho\varphi} = 0 \tag{15}$$

where σ_ρ is the so-called "skin" or tangential stress that often controls in design. The expression for the corresponding stress sensitivity is obtained by taking the total derivative of Eq. (13). One can easily verify that the resulting integrands are regular at $y = 0$. At first, this appears to represent a significant computational advantage over the direct formulation of Eq. (12), which contains singular terms $O(1/s)$. The extent to which this basic difference affects accuracy is examined experimentally in the next section.

Numerical Example

Although the previously derived recovery integrals for design sensitivities are appealing from an analytical standpoint, the ultimate utility of these expressions must be evaluated in a numerical context. Rather than offer an assessment of the approach based on a catalogue of diverse design applications, we seek the basic insight that derives from considering a problem with an analytical solution. With this as a primary objective, numerical results were generated for the infinite elastic plate with an elliptical hole subject to a uniform tension σ_∞ acting at infinity (Fig. 1). For simplicity, the major axis a was chosen as the sole design variable. By restricting the design variable in this way, we were able to obtain exact solutions for the sensitivities and still ensure a nontrivial perturbation of the initial shape. (Details of the analytical differentiation are given in the Appendix.) The availability of the exact solutions made it possible to determine the absolute error of the recovery procedures developed in the previous section. We were also able to quantify the effect of severe stress raisers on accuracy by comparing results for increasing values of the aspect ratio a/b.

All numerical calculations were performed using conforming quadratic boundary elements with approximate displacements calculated from Eq. (3) to ensure an unbiased evaluation. A standard eight-point Gauss formula was employed in evaluating regular integrals. Cauchy principal values were obtained using Kutt's eight-point integration rule for finite-part integrals.[19,20] The unit normal n at integration points was determined by direct shape function differentiation in the usual way. Since the recovery integrals vanish when $x \to \infty$ in the auxiliary problem (the actual problem minus the homogeneous solution associated with the uniform stress at infinity), it was only necessary to discretize the inner elliptical boundary. The boundary elements were spaced at equal increments of the eccentric angle defined in the Appendix, thereby ensuring a suitably graded mesh near the stress concentration. Four progressively finer meshes were employed to determine the rate of convergence for three different aspect ratios: $a/b = 1$, 4, and 8. The corresponding nodal positions are shown in Fig. 2 for $a/b = 4$. To avoid dealing with

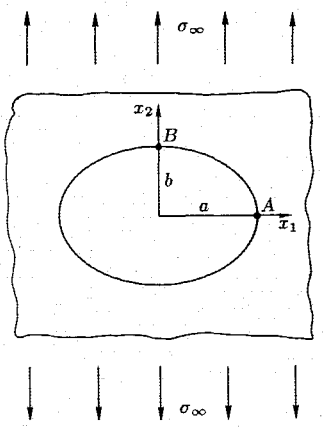

Fig. 1 Two-dimensional infinite plate with elliptical hole.

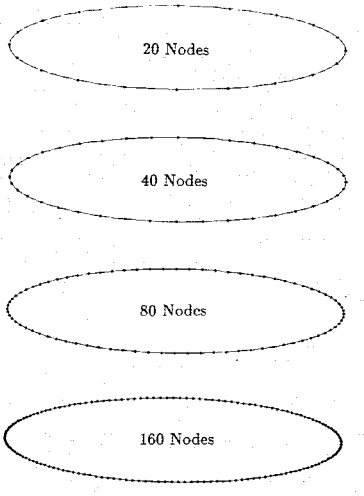

Fig. 2 Boundary element meshes (a/b = 4).

inordinate amounts of data, subsequent error evaluations are confined to the maximum displacement and stress sensitivities at the respective boundary points B and A shown in Fig. 1.

The displacement sensitivities du_2/da from Eq. (9) at the point B were found to be extremely accurate over a broad range of mesh spacings and aspect ratios. Explicit results for $a/b = 1$, 4, and 8 are listed in Table 1. As expected, the maximum error (about 1.1%) occurred with the coarse mesh (20 nodes) and $a/b = 8$. In general, a modest increase in the number of nodes from 20 to 40 reduced the maximum error to less than 0.02%. Furthermore, this error was never significantly greater than the error in the corresponding displacements from Eq. (3).

Next we consider the maximum tangential "skin" stress obtained by evaluating Eq. (10) at the point A in Fig. 1. The corresponding stress sensitivity $d\sigma_{22}/da$ was generated using the direct formulation of Eq. (12), which was derived from Eq. (10). We also determined the stress sensitivity using the alternate eigenfunction extraction procedure described in the previous section. The results shown in Table 2 indicate that both methods converge to the correct results for all three aspect ratios. Although a finer mesh was required to maintain accuracy as the aspect ratio increased, the convergence was extremely rapid in all cases. Even with $a/b = 8$, the error was reduced to less than 4% when the number of nodes was increased from 20 to 40.

Since the direct and eigenfunction extraction techniques yield comparably accurate results, there does not appear to be any compelling reason for selecting one method over the other. At this point, however, we recommend the direct ap-

Table 1 Percent error in displacement sensitivities

a/b	Nodes	u_2	du_2/da
1(3)[a]	20	0.05	0.00
	40	0.00	0.00
	80	0.00	0.00
	160	0.00	0.00
4(9)	20	0.04	0.07
	40	0.01	0.01
	80	0.00	0.00
	160	0.00	0.00
8(17)	20	0.22	1.12
	40	0.02	0.02
	80	0.00	0.00
	160	0.00	0.00

[a]Parentheses indicate stress concentration factor.

Table 2 Percent error in stress sensitivities

a/b	Nodes	σ_{22}	σ_{22}^{b}	$d\sigma_2/da$	$d\sigma_{22}^{b}/da$
1(3)[a]	20	−0.25	−0.28	0.66	0.77
	40	−0.04	−0.04	0.07	0.07
	80	0.00	−0.01	0.01	0.01
	160	0.00	0.00	0.00	0.00
4(9)	20	2.75	3.15	5.42	6.00
	40	0.78	0.85	2.16	2.35
	80	0.11	0.12	0.37	0.41
	160	0.01	0.01	0.05	0.05
8(17)	20	4.11	4.22	6.52	2.95
	40	1.93	2.09	3.49	3.62
	80	0.44	0.48	1.13	1.23
	160	0.06	0.07	0.20	0.21

[a]Parentheses indicate stress concentration factor. [b]Extraction technique.

proach, since it can be extended to three-dimentional problems without introducing major theoretical modifications. A similar generalization of the extraction technique is likely to require a more elaborate theoretical treatment.

Appendix: Analytical Displacement and Stress Sensitivities

Consider a two-dimensional elastic solid with an elliptical hole subject to a uniform stress σ_∞ in the x_2 direction at infinity as indicated in Fig. 1. Let a and b denote the major and minor axes of the elliptical boundary. If θ is the eccentric angle, then the hole geometry can be represented parametrically by the position vector

$$\boldsymbol{r} = a\cos\theta \boldsymbol{e}_1 + b\sin\theta \boldsymbol{e}_2 \tag{A1}$$

where $\boldsymbol{e}_\alpha (\alpha = 1, 2)$ are the unit base vectors. In the case of plane strain, the solution for the displacement $u_\alpha (\alpha = 1, 2)$ given in Ref. 22 can be expressed as

$$u_1 = \frac{\sigma_\infty R}{8\mu}\left[\eta(m-1)\cos\theta + (2F - D)/A\right]$$

$$u_2 = \frac{\sigma_\infty R}{8\mu}\left[\eta(3-m)\sin\theta - (2C - B)/A\right] \tag{A2}$$

where

$$R = (a+b)/2$$

$$\mu = E/2(1+\nu)$$

$$m = (b-a)/(a+b)$$

$$\eta = 3 - 4\nu$$

$$A = 1 + m^2 + 2m\cos 2\theta$$

$$B = (-1 - 2m^2 + m^3)\sin\theta - (2 - m + m^2)\sin 3\theta$$

$$C = (-2 + 2m - 3m^2 + m^3)\sin\theta - (1+m)\sin 3\theta$$

$$D = (1 - 2m^2 + m^3)\cos\theta + (2 - m + m^2)\cos 3\theta$$

$$F = (-m^2 + m^3)\cos\theta + (1-m)\cos 3\theta \tag{A3}$$

After some tedious but straightforward manipulation, the corresponding tangential "skin" stress σ_θ on the hole boundary reduces to

$$\sigma_\theta = \sigma_\infty \frac{1 + 2m - m^2 + 2\cos 2\theta}{1 + m^2 + 2m\cos 2\theta} \tag{A4}$$

If we regard the major axis a as a design variable, then the displacement sensitivities are obtained by differentiating Eq. (A2) as follows:

$$\frac{du_1}{da} = \frac{-b\sigma_\infty}{4\mu(a+b)^2}\left\{R\left[\eta\cos\theta + \frac{A(2F' - D') - A'(2F - D)}{A^2}\right]\right.$$
$$\left. - \frac{b}{(1+m)^2}\left[\eta(m-1)\cos\theta + \frac{2F - D}{A}\right]\right\}$$

$$\frac{du_2}{da} = \frac{b\sigma_\infty}{4\mu(a+b)^2}\left\{R\left[\eta\sin\theta + \frac{A(2C' - B') - A'(2C - B)}{A^2}\right]\right.$$
$$\left. - \frac{b}{(1+m)^2}\left[\eta(m-3)\sin\theta + \frac{2C - B}{A}\right]\right\} \tag{A5}$$

where

$$A' = 2m + 2\cos 2\theta$$

$$B' = m(3m-4)\sin\theta + (1-2m)\sin 3\theta$$

$$C' = (2 - 6m + 3m^2)\sin\theta - \sin 3\theta$$

$$D' = m(3m-4)\cos\theta - (1+2m)\cos 3\theta$$

$$F' = m(3m-2)\cos\theta - \cos 3\theta \tag{A6}$$

Similarly, differentiation of Eq. (A4) gives

$$\frac{d\sigma_\theta}{da} = \frac{\partial\sigma_\theta}{\partial m}\frac{\partial m}{\partial a} = \frac{-2b}{(a+b)^2}\frac{\partial\sigma_\theta}{\partial m} \tag{A7}$$

where

$$\frac{\partial\sigma_\theta}{\partial m} = 2\sigma_\infty[(1-m)(1 + m^2 + 2m\cos 2\theta) - (m + \cos 2\theta)$$
$$\times (1 + 2m - m^2 + 2\cos 2\theta)]/(1 + m^2 + 2m\cos 2\theta)^2 \tag{A8}$$

References

[1]Bennett, J. A. and Botkin, M. E., "Structural Shape Optimization with Geometric Problem Description and Adaptive Mesh Refinement," *AIAA Journal,* Vol. 23, March 1985, pp.458-464.

[2]Shephard, M. S. and Yerry, M. A., "Automatic Finite Element Modeling for Use with Three-dimensional Shape Optimization," *The Optimum Shape: Automated Structural Design,* edited by J. A. Bennett and M. E. Botkin, Plenum, New York, 1986, pp. 113-137.

[3]Barone, M. R. and Caulk, D. A., "Optimal Arrangement of Holes in a Two-Dimensional Heat Conductor by a Special Boundary Integral Method," *International Journal for Numerical Methods in Engineering,* Vol. 18, 1982, pp. 675-685.

[4]Mota Soares, C. A., Rodrigues, H. C., Oliveira, L. M., and Haug, E. J., "Boundary Elements in Shape Optimal Design of Structures," *Boundary Elements,* edited by C. A. Brebbia, Springer-Verlag, New York 1983, pp. 883–889.

[5]Mota Soares, C. A. and Choi, K. K., "Boundary Elements in Shape Optimal Design of Structures," *The Optimum Shape: Automated Structural Design,* edited by J. A. Bennett and M. E. Botkin, Plenum, New York, 1986, pp. 199–231.

[6]Choi, J. H. and Kwak, B. M., "Boundary Integral Equation Method for Shape Design Sensitivity Analysis," *Computer Aided Optimal Design: Structural and Mechanical Systems,* edited by C. A. Mota Soares, NATO/NASA/NSF/USAF Advanced Study Institute, 1986.

[7]Meric, R. A., "Boundary Element in Shape Design Sensitivity Analysis of Thermoelastic Solids," *Computer Aided Optimal Design: Structural and Mechanical Systems,* edited by C. A. Mota Soares, NATO/NASA/NSF/USAF Advanced Study Institute, 1986.

[8]Wu, S. J., "Applications of the Boundary Element Method for Structural Shape Optimization," Ph.D. Thesis, The University of Missouri, Columbia, MO, 1986.

[9]Kane, J. H., "Optimization of Continuum Structures Using a Boundary Element Formulation," Ph.D. Thesis, The University of Connecticut, 1986.

[10]Haug, E. J., Choi, K. K., and Komkov, V., *Design Sensitivity Analysis of Structural Systems,* Academic Press, 1986.

[11]Dems, K. and Mroz, Z., "Variational Approach by Means of Adjoint Systems to Structural Optimization and Sensitivity Analysis-II, Structure Shape Variation," *International Journal of Solids and Structures,* Vol. 20, No. 6, 1984, pp. 527–552.

[12]Braibant, V. and Fleury, C., "Shape Optimal Design, A Performing C.A.D. Oriented Formulation," AIAA Paper 84-0857, May 1984.

[13]Yang, R. J. and Botkin, M. E., "Comparison Between the Variational and Implicit Differentiation Approaches to Shape Design Sensitivities," *AIAA Journal,* Vol. 24, June 1986, pp. 1027–1032.

[14]Bennett, J. A. and Botkin, M. E., *The Optimum Shape: Automated Structural Design,* Plenum, New York, 1986.

[15]Cruse, T. A. and Vanburen, W., "Three-Dimensional Elastic Stress Analysis of a Fracture Specimen with an Edge Crack," *International Journal of Fracture Mechanics,* Vol. 7, No. 1, March 1971, pp. 1–15.

[16]Barone, M. R. and Robinson, A. R., "Determination of Elastic Stresses at Notches and Corners by Integral Equations," *International Journal of Solids and Structures,* Vol. 8, 1972, pp. 1319–1338.

[17]Vasilopoulos, D., personal communication, 1986.

[18]Banerjee, P. K. and Butterfield, R., *Boundary Element Methods in Engineering Science,* McGraw-Hill, New York, 1981.

[19]Brebbia, C. A., Telles, J. C. F., and Wrobel, L. C., *Boundary Element Techniques,* Springer-Verlag, New York 1984.

[20]Kutt, H. R., "Quadrature Formulae for Finite Part Integrals," The National Research Institute for Mathematical Sciences, Pretoria, 1975.

[21]Aksentian, O. K., "Singularities of the Stress-Strain State of a Plate in the Neighborhood of an Edge," *Prikladnaya Matematika y Mekanika,* Vol. 31, 1967, pp. 193–202.

[22]Muskhelishvili, N. I., *Some Basic Problems of the Mathematical Theory of Elasticity,* P. Noordhoff Ltd., Groningen, the Netherlands, 1963.

From the AIAA Progress in Astronautics and Aeronautics Series...

ORBIT-RAISING AND MANEUVERING PROPULSION: RESEARCH STATUS AND NEEDS—v. 89

Edited by Leonard H. Caveny, Air Force Office of Scientific Research

Advanced primary propulsion for orbit transfer periodically receives attention, but invariably the propulsion systems chosen have been adaptations or extensions of conventional liquid- and solid-rocket technology. The dominant consideration in previous years was that the missions could be performed using conventional chemical propulsion. Consequently, major initiatives to provide technology and to overcome specific barriers were not pursued. The advent of reusable launch vehicle capability for low Earth orbit now creates new opportunities for advanced propulsion for interorbit transfer. For example, 75% of the mass delivered to low Earth orbit may be the chemical propulsion system required to raise the other 25% (i.e., the active payload) to geosynchronous Earth orbit; nonconventional propulsion offers the promise of reversing this ratio of propulsion to payload masses.

The scope of the chapters and the focus of the papers presented in this volume were developed in two workshops held in Orlando, Fla., during January 1982. In putting together the individual papers and chapters, one of the first obligations was to establish which concepts are of interest for the 1995-2000 time frame. This naturally leads to analyses of systems and devices. This open and effective advocacy is part of the recently revitalized national forum to clarify the issues and approaches which relate to major advances in space propulsion.

Published in 1984, 569 pp., 6 × 9, illus., $49.95 Mem., $69.95 List

TO ORDER WRITE: Publications Dept., AIAA, 370 L'Enfant Promenade S.W., Washington, D.C. 20024-2518